

## Properties of dawsonite conversion film on AZ31 magnesium alloy

CHEN Jun, SONG Ying-wei, SHAN Da-yong, HAN En-hou

State Key Laboratory for Corrosion and Protection, Institute of Metal Research,  
Chinese Academy of Sciences, Shenyang 110016, China

Received 23 September 2009; accepted 25 December 2010

**Abstract:** An environmentally friendly method for synthesizing a dawsonite conversion film was developed to improve the corrosion resistance of AZ31 Mg alloy. The film was prepared by two steps: the AZ31 alloy was first immersed in an  $\text{Al}_2(\text{SO}_4)_3$  solution venting  $\text{CO}_2$  gas to form a precursor film, and then the precursor film was treated in a  $\text{Na}_2\text{CO}_3$  solution dissolved with Al to obtain the dawsonite film. The surface morphology of the conversion film was observed with an environmental scanning electronic microscope. The chemical composition of the conversion film was analyzed by energy dispersive X-ray spectroscopy and X-ray diffractometry. Electrochemical and immersion tests were carried out to evaluate the protection effect of the conversion film on AZ31 alloy. There are some network-like cracks on the surface of the film. The conversion film is mainly composed of dawsonite  $\text{NaAlCO}_3(\text{OH})_2$ ,  $\text{Al}(\text{OH})_3$  and  $\text{Al}_5(\text{OH})_{13}(\text{CO}_3)\cdot 5\text{H}_2\text{O}$ , which can increase the corrosion potential and reduce the corrosion current density of the Mg substrate. After immersion tests, the film almost keeps intact, except for the localized narrow areas with several corrosion pits, while the bare material undergoes serious general corrosion. It is indicated that the dawsonite film can provide good protection to the magnesium alloy.

**Key words:** magnesium alloy; dawsonite; conversion film; corrosion

### 1 Introduction

Magnesium and its alloys have become critical to engineers nowadays due to their special properties, such as low density, high specific strength, good castability, high damping capacity, good recycling potential and abundant resources[1]. These properties make them ideal candidates for lightweight engineering applications, especially in the automotive industry, electronic products, aerospace industry, etc[2–3]. However, the poor corrosion resistance of Mg alloys limits their applications[4–5]. Scientists try to develop various coatings such as chemical conversion coatings[3, 6–10], anodized coatings[11–12], organic coatings[13–14], as well as metal coatings[15–16] to enhance the corrosion resistance of Mg alloys. Typically, the chemical conversion coatings are most widely used because they are easy to perform and cost-effective[17]. Chromate conversion coatings (CCC)[6] provide highly effective corrosion protection, but environmental regulations are increasingly restricting their use. Several promising chromate-free conversion coatings, including phosphate-permanganate[7], stannate[8] and rare earth[3, 9–10],

particularly cerium-based and other coatings, are available. However, it takes into account the limitation of rare earth reserves and the environmental problems associated with heavy metal ions and phosphorus. Moreover, some ions from the above mentioned conversion coatings may contaminate the magnesium melt and make the recycling of Mg products more difficult[1, 18–21]. Hence, none of these methods is perfect. The development of a simple and environmentally friendly approach for growing anti-corrosion film on Mg alloys is a considerable challenge. Thus, various studies have been carried out to search for appropriate coatings.

Aluminium is a primary alloy element for the AZ series magnesium alloys, and it has a beneficial effect on the corrosion resistance of magnesium[22]. This work aims at preparing an environmentally friendly aluminium-based chemical conversion film with good corrosion resistance on AZ31 Mg alloy.

### 2 Experimental

#### 2.1 Fabrication of dawsonite conversion film

The material used in this study was AZ31 Mg alloy

with a size of 25 mm × 50 mm × 2 mm. The surface of the samples was ground with 2000 grit SiC sand paper. Samples were firstly immersed in the pretreatment solution at room temperature (RT) for 1 h to form a precursor film, and then the precursor film was treated in the post treatment solution at 60 °C for 2 h to obtain the dawsonite conversion film. The pretreatment solution was 0.01 mol/L  $\text{Al}_2(\text{SO}_4)_3 \cdot 18\text{H}_2\text{O}$  with continually bubbled  $\text{CO}_2$  gas. The post treatment solution was prepared by dissolving an Al panel in 0.5 mol/L  $\text{Na}_2\text{CO}_3$  solution until the saturation of Al compounds (a small amount of precipitation appeared).

## 2.2 Characterization

The morphology of the films and corroded samples was observed using a Philips XL30 type environmental scanning electronic microscope (ESEM) equipped with an energy dispersive X-ray spectrum (EDS). The constituent of the films was measured by a Philips PW1700 X-ray diffraction (XRD) with Cu target. The XRD pattern was analyzed with MDI Jade 5.0 software.

An EG&G Potentiostat model 273 was utilized to study the electrochemical corrosion behavior. Three-electrode system was applied: the working electrode exposed a surface area of 100 mm<sup>2</sup>; a saturated calomel electrode (SCE) and a platinum plate used as reference electrode and auxiliary electrode, respectively. The polarization measurements started after an initial delay of 300 s. The potential scanned from −300 to +200 mV vs open current potential (OCP) with a scanning rate of 0.5 mV/s. Electrochemical impedance spectroscopy (EIS) measurements were performed using a model 5210 lock-in amplifier coupled with a potentiostat model 273. EIS plots were acquired in a frequency range from 100 kHz to 10 mHz with an AC wave of 5 mV. An initial delay of 300 s was set to ensure a stable testing system before undertaking the experiment. The immersion tests were performed according to the GB Standard 10124—88 of China. 0.1 mol/L NaCl aqueous solution was used as the electrolyte for the electrochemical and immersion tests. All the tests were performed at RT.

## 3 Results and discussion

### 3.1 Morphology of films

Figure 1 shows the SEM micrographs of the samples with precursor and dawsonite film. The SEM morphology of the precursor film on AZ31 alloy shown in Fig.1(a) reveals a continuous coating with cracks. Fig.1(b) depicts the dawsonite film with network-like cracks. Compared with the precursor film, the surface

cracks were reduced and the flaw size was refined due to the post treatment in  $\text{Na}_2\text{CO}_3$  solution containing Al compounds. The chemical composition of the films was determined by EDS and listed in Table 1. It discloses that the precursor film was mainly composed of Al, O and S with a small amount of Mg, whereas the major elements in the final film were Al, O, and C, the content of Mg and S decreased and Na appeared. The variation in C concentration reveals that the precursor film changed to compounds containing C after post treatment.

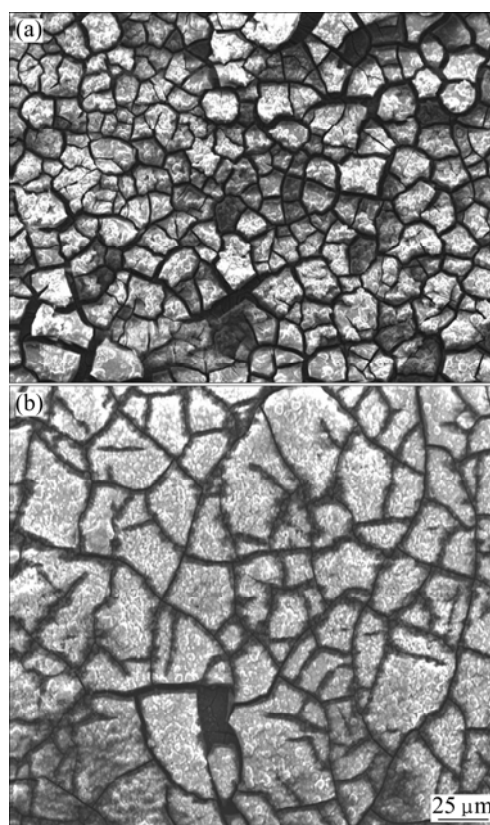


**Fig.1** SEM images of samples with precursor film (a) and final film (b)

**Table 1** Compositions of precursor and final films (mass fraction, %)

Sample	O	Mg	Al	S	C	Na
Precursor	53.36	03.46	36.05	06.94	—	—
Final film	42.58	00.70	34.06	01.07	17.22	04.36

### 3.2 XRD analysis of films

The XRD patterns of the precursor and final films formed on the surface of AZ31 alloy are shown in Fig.2. The major phases existing in the precursor film were  $\text{Mg}(\text{OH})_2(\text{SO}_4)_2 \cdot 3\text{H}_2\text{O}$  and  $\text{AlO}(\text{OH})$ . The final film was composed of  $\text{NaAlCO}_3(\text{OH})_2$  dawsonite compound,  $\text{Al}(\text{OH})_3$  and  $\text{Al}_5(\text{OH})_{13}(\text{CO}_3) \cdot 5\text{H}_2\text{O}$ .

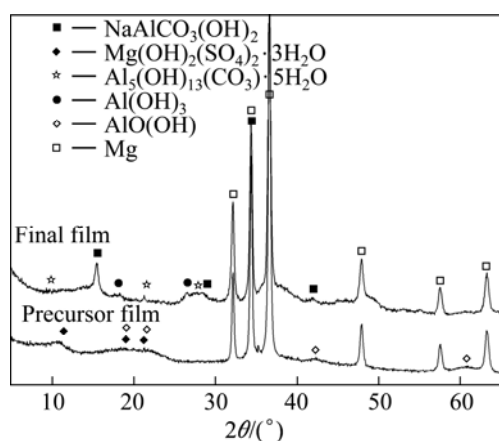


Fig.2 XRD patterns of films formed on surface of AZ31 alloy

### 3.3 Corrosion behavior of dawsonite film

Figure 3(a) shows the curves of free corrosion potential ( $\varphi_{\text{corr}}$ ) as a function of time for the AZ31 substrate and its dawsonite film in 0.1 mol/L NaCl solution. The  $\varphi_{\text{corr}}$  of the substrate rose continuously, then slightly sloped down, and finally sustained a stable level of  $-1.558$  V(vs SCE) with increasing immersion time. It implies that a protective  $\text{Mg}(\text{OH})_2$  corrosion product film was formed immediately on the AZ31 substrate, and then the film ruptured after being soaked for 3 115 s. Finally, the rupture and formation of the corrosion products film reached a dynamic equilibrium. The  $\varphi_{\text{corr}}$  of the dawsonite film rapidly increased from  $-1.736$  to  $-1.505$  V(vs SCE) at 730 s in the initial stage of immersion, and then kept stable with a sudden interruption at 4 570 s, and finally fluctuated in a small range, indicating the local failure of the film and the formation of corrosion products. It is obvious that the  $\varphi_{\text{corr}}$  of AZ31 alloy with film was always more positive than that of the substrate, which indicates that the AZ31 substrate became more stable after being deposited with the dawsonite film.

Polarization curves are demonstrated in Fig.3(b). There was great difference at the anodic sides of the two curves. In the case of AZ31 alloy, the corrosion current density quickly increased with increasing potential, indicating the active dissolution of Mg substrate. Differently, the anodic side of the coated alloy exhibited a large passivation region and the breakdown potential  $\varphi_b$  was about  $-1.31$  V( vs SCE). This result indicates that the dawsonite film can greatly inhibit the corrosion of Mg substrate. Once the anodic potential reached the film breakdown potential, the sample corroded quickly, implying that the film is sensitive to pitting corrosion. The electrochemical parameters of the alloy with and without film are listed in Table 2. It is clear that the dawsonite film significantly improves the corrosion resistance of AZ31 alloy in view that  $J_{\text{corr}}$  value was decreased by about two orders of magnitude.

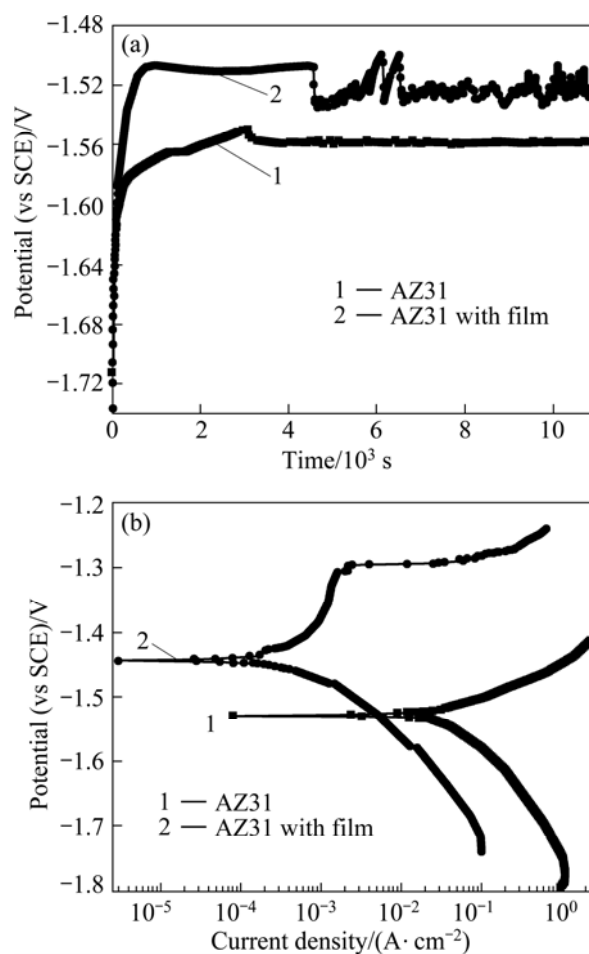


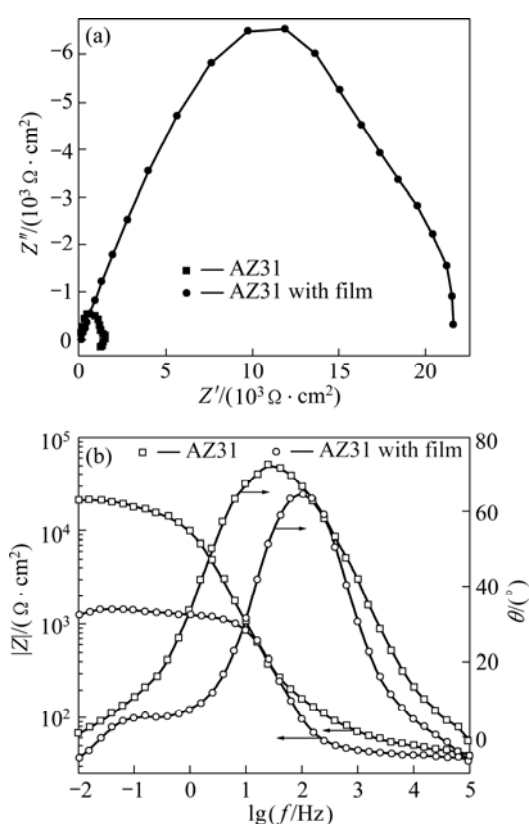
Fig.3 Potential vs time curves (a) and polarization curves (b) of AZ31 alloy with and without film in 0.1 mol/L NaCl solution

Table 2 Electrochemical parameters of alloy with and without film in 0.1 mol/L NaCl solution

Sample	$\varphi_{\text{corr}}$ (vs SCE)/V	$J_{\text{corr}}$ /( $\text{A}\cdot\text{cm}^{-2}$ )
AZ31 substrate	$-1.527$	$5.410\times 10^{-5}$
AZ31 with film	$-1.441$	$4.679\times 10^{-7}$

The corrosion behavior of the AZ31 alloy with and without film was investigated with EIS measurements (Fig.4). The Nyquist plot for the AZ31 substrate consisted of three loops, one high frequency capacitive loop, one medium frequency capacitive loop and one short low frequency inductive loop. The high frequency capacitive loop is due to the contribution of electric double layer at the interface of substrate and solution; the medium frequency capacitive loop relates to the adsorption of corrosion products on the AZ31 surface[23], BARIL et al[24] and ANIK and CELNKTEN[25] also suggested that this loop originates from the diffusion through a porous solid film, and the low frequency inductive loop is attributed to the corrosion nucleation in the initiation stage of localized

corrosion. The existence of inductive loop indicates that there are corrosion pits on the surface of Mg substrate. The plot for the coated sample contains only one capacitive loop. It implies that the coating is compact and undamaged. In addition, the diameter of the plot is much larger than that of the substrate. According to the Bode plot of  $|Z|$  vs frequency, it is found that the  $|Z|$  value changes from  $1.46 \times 10^3$  for the AZ31 substrate to  $2.21 \times 10^4 \Omega \cdot \text{cm}^2$  for the dawsonite film coated sample. Higher  $|Z|$  value represents better corrosion resistance[23]. Thus, the conversion film can enhance the corrosion resistance of AZ31 alloy in 0.1 mol/L NaCl solution.



**Fig.4** EIS results of AZ31 alloy with and without film in 0.1 mol/L NaCl solution: (a) Nyquist plots; (b) Bode plots

EIS plots can be equivalent to the circuits as shown in Fig.5, which can be applied to simulate the impedance plots of the bare AZ31 and coated sample.  $R_s$  is the solution resistance;  $R_{ct}$  is the charge transfer resistance;  $Q_f$  is the capacity of conversion film on AZ31 alloy and  $Q_{dl}$  represents the electric double layer capacity. The constant phase element ( $Q$ ) is used to compensate for

the non-homogeneity in the system[23].  $Q$  is defined by two values,  $Y_0$  and  $n$ . If  $n$  is equal to 1,  $Q$  is identical to a capacitor.  $C_f$  and  $R_f$  represent the capacity and resistance of the corrosion products film on AZ31 alloy, respectively.  $R_L$  and  $L$  represent the inductance resistance and inductance, respectively, and are used to describe the low frequency inductive loop, implying the initiation of pitting corrosion[23]. The capacity and resistance of the conversion film on AZ31 alloy are characterized by  $Q_f$  and  $R_f$ , respectively. The EIS fitting results are listed in Table 3. The  $R_f$  for the coated sample is about two orders of magnitude of the  $R_f$  for the bare alloy, which indicates that the corrosion resistance of the dawsonite film is much better than that of the corrosion products film formed on the AZ31 substrate surface.

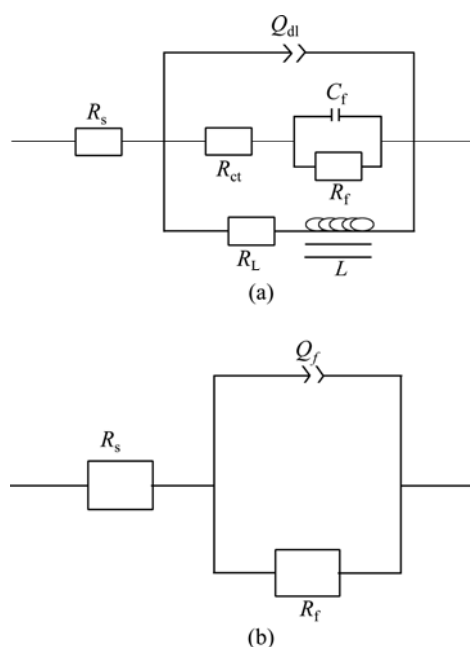


**Fig.5** Equivalent circuits of EIS plots for (a) bare AZ31 alloy and (b) AZ31 alloy with film

**3.4 Corrosion morphologies of dawsonite film**

Figure 6 shows the optical morphologies of the AZ31 specimens with and without film after 2.5, 24 and 48 h immersion tests, respectively. After 2.5 h, severe pitting corrosion occurred on the bare material, as marked in Fig.6(a). However, the first corrosion pit initiated on the specimen with dawsonite film until 2.5 h later, as shown in Fig.6(d). It can be seen that the corrosion did not present at other areas and only expanded around the initial pits. After 48 h immersion

**Table 3** Fitting results of EIS plots for AZ31 with and without film

Sample	$R_s/(\Omega \cdot \text{cm}^2)$	$Y_0/(10^{-6} \Omega^{-1} \cdot \text{cm}^{-2} \cdot \text{s}^{-1})$	$n$	$R_{ct}/(\Omega \cdot \text{cm}^2)$	$C_f/(\mu\text{F} \cdot \text{cm}^{-2})$	$R_f/(\Omega \cdot \text{cm}^2)$	$L/(\text{H} \cdot \text{cm}^2)$	$R_L/(\Omega \cdot \text{cm}^2)$
Bare AZ31 alloy	39.05	11.74	0.921 4	1 237	6 306	236.2	79 060	6 245
AZ31 alloy with film	45.81	12.32	0.813			20 190		

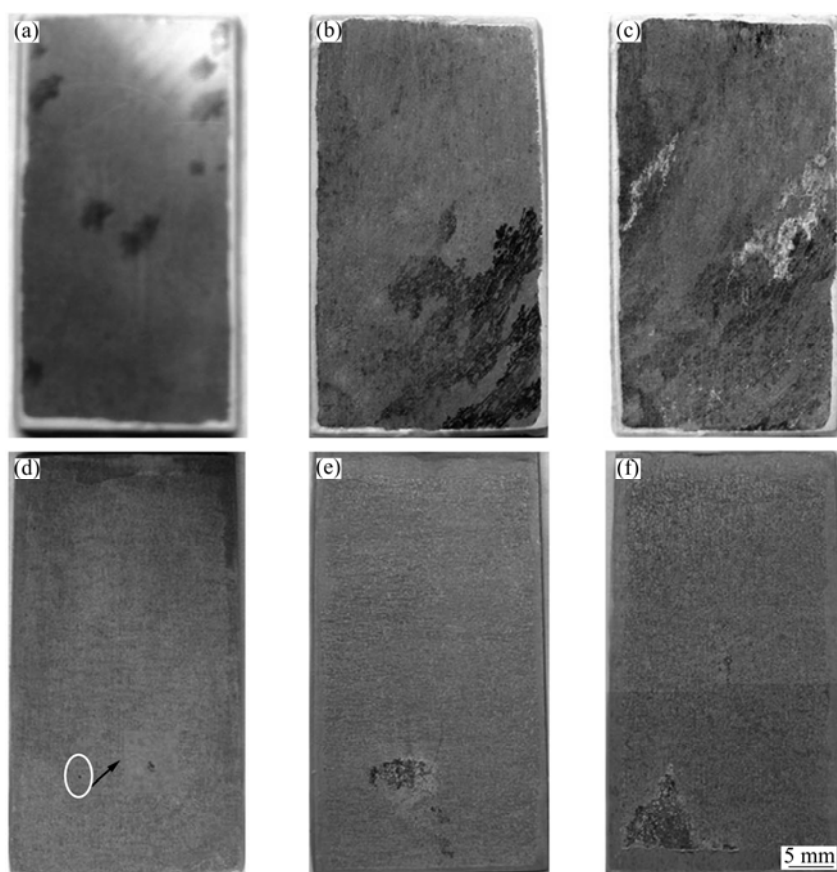


**Fig.6** Optical morphologies of substrates (a, b, c) and coated specimens (d, e, f) after immersion tests for 2.5 h, 24 h and 48 h in 0.1 mol/L NaCl, respectively

test, the bare material underwent serious general corrosion (Fig.6(c)), while the majority of the coated sample was not attacked except for the localized narrow areas (Fig.6(f)). It is in accordance with the result of polarization curves that the coated sample is susceptible to pitting corrosion and the bare alloy can not resist to general corrosion. The optical corrosion morphologies also indicate that the corrosion resistance of the coated alloy was superior to that of the Mg substrate.

SEM corrosion morphology of the dawsonite film after immersed in 0.1 mol/L NaCl solution for different time is shown in Fig.7. There was one corrosion pit appearing on the surface of the film after 2.5 h immersion, and the size of the corrosion pit gradually increased with increasing immersion time. The film lost its typical dawsonite film surface morphology after corrosion, and a different layer of insoluble corrosion products was deposited on the pit area. However, other regions still kept intact even after 48 h immersion (Fig.7(d)).

EDS test was carried out in the rectangle regions as marked in Fig.7 to study the chemical composition of the films after immersion test, and the results are listed in

Table 4. It can be observed that there existed slight change in the content of the elements in the intact area of the film, which agrees with the images as shown in Fig.7(d) compared with the film without immersion as listed in Table 1. However, the content of Mg increased greatly in the corrosion pits. Usually, in aqueous solution, the surface layer of magnesium can react with water to form magnesium hydroxide ( $Mg(OH)_2$ ). When the conversion film ruptures and the Mg substrate is exposed, more and more  $Mg(OH)_2$  is deposited in the corrosion pits with increasing immersion time. Correspondingly, the content of Mg increases, while that of C reduces from 20.37% to 13.52%.

**Table 4** Compositions of dawsonite film after immersion in 0.1 mol/L NaCl solution for different time intervals (molar fraction, %)

Position	O	Mg	Al	C	Na	Cl
2.5 h pit	41.41	31.66	3.52	20.37	–	3.04
24 h pit	42.23	34.23	5.33	16.69	1.51	–
48 h pit	44.33	36.55	4.41	13.52	1.19	–
48 h intact film	41.76	2.79	41.73	11.04	–	–

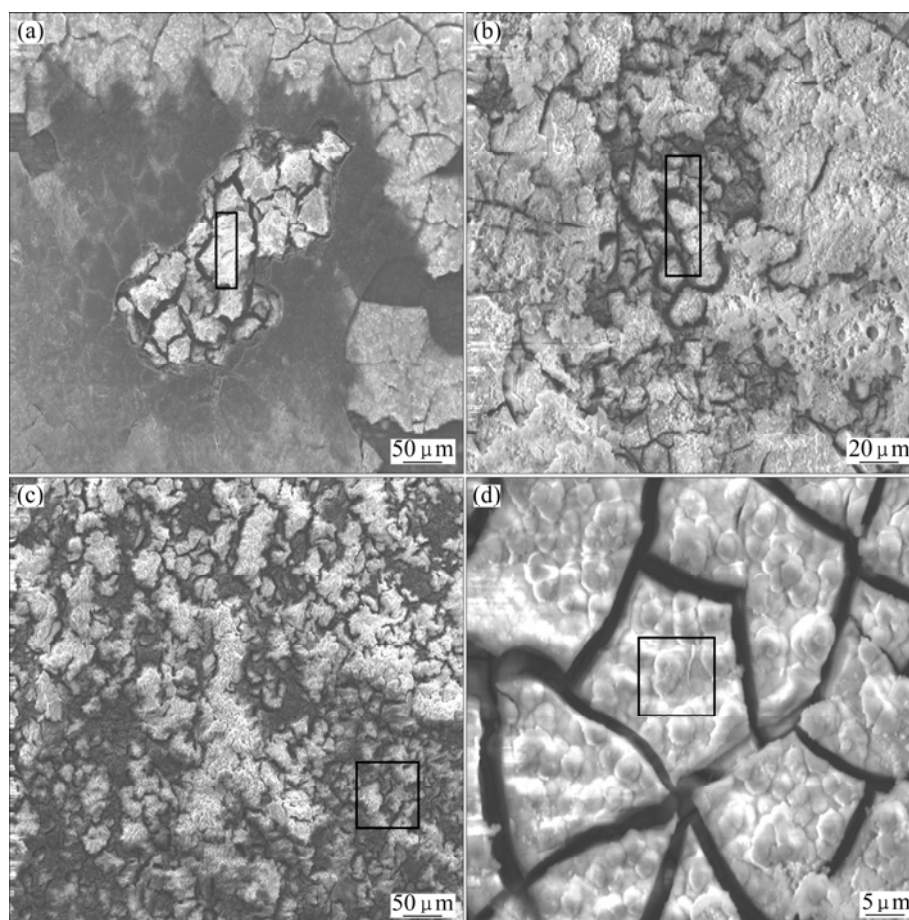


Fig.7 SEM images of coated samples after immersion tests for 2.5 h (a), 24 h (b) and 48 h (c, d)

## 4 Conclusions

1) An environmentally friendly method for synthesizing dawsonite conversion film is developed to improve the corrosion resistance of AZ31 Mg alloy. The film is mainly composed of  $\text{NaAlCO}_3(\text{OH})_2$ ,  $\text{Al}(\text{OH})_3$  and  $\text{Al}_5(\text{OH})_{13}(\text{CO}_3) \cdot 5\text{H}_2\text{O}$ .

2) The conversion film can increase the corrosion potential ( $\phi_{\text{corr}}$ ) and decline the corrosion current density ( $J_{\text{corr}}$ ) of the substrate by about two orders of magnitude. The anodic polarization curve of the coated alloy exhibits a large passivation region. It is indicated that this film can provide good protection to the Mg alloy.

3) After immersion tests, the film almost keeps intact, except for the localized narrow areas with some corrosion pits, while the bare material undergoes serious general corrosion.

## References

- [1] GRAY J E, LUAN B. Protective coatings on magnesium and its alloys—A critical review [J]. *Journal of Alloys and Compounds*, 2002, 336(1–2): 88–113.
- [2] BEN HAMU G, ELIEZER D, WAGNER L. The relation between

severe plastic deformation microstructure and corrosion behavior of AZ31 magnesium alloy [J]. *Journal of Alloys and Compounds*, 2009, 468(1–2): 222–229.

- [3] RUDD A L, BRESLIN C B, MANSFELD F. The corrosion protection afforded by rare earth conversion coatings applied to magnesium [J]. *Corrosion Science*, 2000, 42(2): 275–288.
- [4] SONG G, ATRENS A, St JOHN D, NAIRN J. The electrochemical corrosion of pure magnesium in 1N NaCl [J]. *Corrosion Science*, 1997, 39(5): 855–875.
- [5] MAKAR G L, KRUGER J. Corrosion studies of rapidly solidified magnesium alloys [J]. *Journal of the Electrochemical Society*, 1990, 137(2): 414–421.
- [6] CHIDAMBARAM D, CLAYTON C R, HALADA G P. The role of hexafluorozirconate in the formation of chromate conversion coatings on aluminum alloys [J]. *Electrochimica Acta*, 2006, 51(14): 2862–2871.
- [7] ZHOU Wan-qiu, SHAN Da-yong, HAN En-hou, KE Wei. Structure and formation mechanism of phosphate conversion coating on die-cast AZ91D magnesium alloy [J]. *Corrosion Science*, 2008, 50(2): 329–337.
- [8] ZUCCHI F, FRIGNANI A, GRASSI V, TRABANELLI G, MONTOCELLI C. Stannate and permanganate conversion coatings on AZ31 magnesium alloy [J]. *Corrosion Science*, 2007, 49(12): 4542–4552.
- [9] MONTEMOR M F, SIMOES A M, CARMEZIM M J. Characterization of rare-earth conversion films formed on the AZ31 magnesium alloy and its relation with corrosion protection [J]. *Applied Surface Science*, 2007, 253(16): 6922–6931.
- [10] ARDELEAN H, FRATEUR I, MARCUS P. Corrosion protection of

- magnesium alloys by cerium, zirconium and niobium-based conversion coatings [J]. Corrosion Science, 2008, 50(7): 1907–1918.
- [11] SHI Zhi-ming, SONG Guang-ling, ATRENS A. The corrosion performance of anodised magnesium alloys [J]. Corrosion Science, 2006, 48(11): 3531–3546.
- [12] ZHANG R F, XIONG G Y, HU C Y. Comparison of coating properties obtained by MAO on magnesium alloys in silicate and phytic acid electrolytes [J]. Current Applied Physics, 2010, 10(1): 255–259.
- [13] KIM J, WONG K C, WONG P C, KULINICH S A, METSON J B, MITCHELL K A R. Characterization of AZ91 magnesium alloy and organosilane adsorption on its surface [J]. Applied Surface Science, 2007, 253(9): 4197–4207.
- [14] SHI Hong-wei, LIU Fu-chun, HAN En-hou. Corrosion protection of AZ91D magnesium alloy with sol-gel coating containing 2-methyl piperidine [J]. Progress in Organic Coatings, 2009, 66(3): 183–191.
- [15] HUANG C A, WANG T H, WEIRICH T, NEUBERT V. Electrodeposition of a protective copper/nickel deposit on the magnesium alloy (AZ31) [J]. Corrosion Science, 2008, 50(5): 1385–1390.
- [16] SONG Ying-wei, SHAN Da-yong, HAN En-hou. High corrosion resistance multilayer nickel coatings on AZ91D magnesium alloys [J]. Surface Engineering, 2007, 23(5): 329–333.
- [17] ELSENTRIECY H H, AZUMI K, KONNO H. Effects of pH and temperature on the deposition properties of stannate chemical conversion coatings formed by the potentiostatic technique on AZ91 D magnesium alloy [J]. Electrochimica Acta, 2008, 53(12): 4267–4275.
- [18] HANKO G, ANTREKOWITSCH H, EBNER P. Recycling automotive magnesium scrap [J]. Journal of the Minerals Metals and Materials Society, 2002, 54(2): 51–54.
- [19] JAVAID A, ESSADIQI E, BELL S, DAVIS B. Literature review on magnesium recycling [C]//LUO A A, NEEL A N R, BEALS R S. Magnesium Technology 2006. San Antonio, America, 2006: 7–12.
- [20] YU Bing-lun, LIN Jun-kai, UAN Jun-yen. Recent studies on applications of carbonic acid solution for developing conversion coating on Mg alloy [J]. Transactions of Nonferrous Metals Society of China, 2010, 20(7): 1331–1339.
- [21] LI W P, WANG X M, ZHU L Q, LI W. Formation mechanism of an aluminium-based chemical conversion coating on AZ91D magnesium alloy [J]. International Journal of Minerals, Metallurgy and Materials, 2010, 17(5): 641–647.
- [22] LIANG J, GUO B, TIAN J, LIU H W, ZHOU J F, LIU W M, XU T. Effects of NaAlO<sub>2</sub> on structure and corrosion resistance of microarc oxidation coatings formed on AM60B magnesium alloy in phosphate-KOH electrolyte [J]. Surface Coating Technology, 2005, 199(2–3): 121–126.
- [23] CAO Chu-nan, ZHANG Jian-qing. Introduction of Electrochemical Impedance Spectroscopy [M]. Beijing: Science Press, 2002. (in Chinese)
- [24] BARIL G, GALICIA G, DESLOUIS C, PEBERE N, TRIBOLLET VIVIER B V. An impedance investigation of the mechanism of pure magnesium corrosion in sodium sulphate solution [J]. Journal of the Electrochemical Society, 2007, 154(2): C108–C113.
- [25] ANIK M, CELIKTEN G. Analysis of the electrochemical reaction behavior of alloy AZ91 by EIS technique in H<sub>3</sub>PO<sub>4</sub>/KOH buffered K<sub>2</sub>SO<sub>4</sub> solutions [J]. Corrosion Science, 2007, 49(4): 1878–1894.

## AZ31 镁合金表面碳钠铝石转化膜的性能

陈君, 宋影伟, 单大勇, 韩恩厚

中国科学院 金属研究所 金属腐蚀与防护国家重点实验室, 沈阳 110016

**摘要:** 开发一种环境友好的方法合成碳钠铝石转化膜以提高 AZ31 镁合金的耐蚀性。该膜由两步法制得: 首先将 AZ31 合金浸泡在一直通 CO<sub>2</sub> 气体的 Al<sub>2</sub>(SO<sub>4</sub>)<sub>3</sub> 溶液中, 获得前躯体膜; 随后将该前躯体膜浸泡在溶有 Al 的 Na<sub>2</sub>CO<sub>3</sub> 溶液中以获得碳钠铝石膜。通过环境扫描电镜观察转化膜的表面形貌, 并利用 EDS 能谱和 X 射线衍射分析其化学成分。采用电化学和浸泡实验来评价该转化膜对 AZ31 合金的防护作用。结果表明: 膜的表面存在网状裂痕, 其成分主要为碳钠铝石 NaAlCO<sub>3</sub>(OH)<sub>2</sub>、Al(OH)<sub>3</sub> 和 Al<sub>5</sub>(OH)<sub>13</sub>(CO<sub>3</sub>)<sub>2</sub>·5H<sub>2</sub>O。该膜能提高 Mg 基体的自腐蚀电位, 并减少其腐蚀电流密度。浸泡实验后, 除了局部小区域有个别点蚀坑外, 膜基本保持完整; 而基体却腐蚀严重。说明碳钠铝石转化膜能很好地保护镁合金。

**关键词:** 镁合金; 碳钠铝石; 转化膜; 腐蚀

(Edited by FANG Jing-hua)